Mapping Depth at Select Positions in Dana Point Harbor Through Three Distinct Methods

Sebastian Heredia[1], John Simon[1], Georgia Tai[1], Simone Yang[1], *Team 35*, *Section 3*, *May 9th*, *2025*

***Abstract*—This report outlines the design, development, and deployment of an autonomous surface vehicle (ASV) built for the E80: Experimental Engineering course for Sophomores at Harvey Mudd College. The robot was tasked with collecting underwater depth data at Dana Point Harbor, specifically Baby Beach, using a combination of electrical and mechanical depth sensing systems. The ASV was equipped with a motor that enabled lowering and raising of a winch weight, a Hall effect sensor to count winch spool revolutions, and a pressure sensor. Although the robot was unable to autonomously navigate to desired waypoints during deployment, all measuring systems successfully ran. To collect data, the ASV was manually moved to each waypoint by Simone Yang. The robot collected data at 11 positions between the dock and the shore, spanning a distance of 40m due North. While exact values varied, all three methods indicated that depth initially increased rapidly with distance from the shore before leveling off at positions beyond 5m from the shoreline. A paired t-test revealed no statistically significant difference between the pressure and Hall effect sensor measured data ($P = 0.742$). Conversely, additional t-tests revealed the motor and Hall effect sensor were statistically different ($P = 2.06 \times 10^{-5}$) as well as the motor and pressure sensor ($P = 2.49 \times 10^{-4}$). Ultimately, it was concluded that the pressure and Hall effect sensors could effectively be used for high-resolution depth mapping of waters up to 5m deep, but that further calibration would be needed to refine the motor depth measuring method.**

I. Introduction

The goal of the project was to explore the potential of using electrical and mechanical depth measuring methods to determine the water depth from an autonomous surface vehicle (ASV) to the ocean floor as an alternative to pressure-based depth sensors. The ASV was equipped with three sensors: a motor serving as a winch actuator and generator, a Hall effect sensor to track winch spool rotations, and a pressure sensor. In addition to the three depth measuring sensors, an electromagnet was implemented to hold the winch weight in place in between trials to prevent overusing the motor to hold the weight in a raised position.

The mechanical integration of each sensor and interfacing between sensors was critical to the robot's function. Below, *Figure 1a* at left shows the setup of the sensors on the robot frame while *Figure 1b* at right shows the electromagnet fixed to the robot frame by a screw.

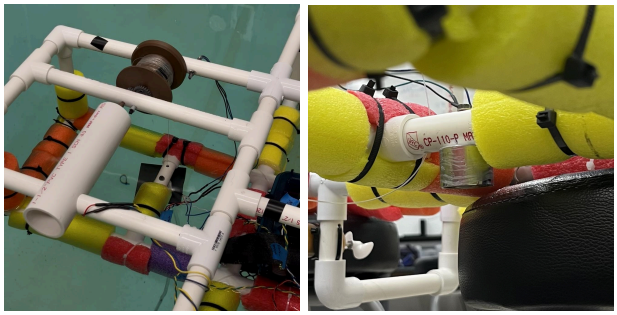

Figure 1a (left): All three sensors—Hall effect, motor, and pressure—were connected via the winch device. The Hall effect sensor mechanically measured spool rotations and the motor served to raise the winch weight while electrically measuring changes in voltage to determine depth. Moreover, the open end of the pressure sensor tube was connected to the winch weight and was lowered during each trial.

Figure 1b (right): The electromagnet was waterproofed with Parafilm and served as a mechanism to hold the winch weight in place. When the electromagnet was deactivated, the winch weight lowered due to gravity.

The common component between all three sensors was the winch—a lifting device consisting of a steel plate attached to a fishing line wound around a horizontally rotating spool. Importantly, the open end of the pressure sensor tube was fixed to the winch weight, such that for each trial the pressure sensor measured depth alongside the winch weight. Thus, for a given trial, the electromagnet was first deactivated, allowing the weight and pressure sensor tube to lower to the ocean floor as a result of gravity. Then, when powered, the motor sensor acted as an actuator, converting energy into rotational motion to rotate the spool to reel up the winch weight and pressure sensor tube apparatus.

The design for interfacing sensors on the robot to take depth measurements was based around the winch. Assuming a constant water density, the pressure sensor measured depth based on a known relationship between water pressure and depth. In contrast, a Hall effect sensor was used to mechanically count winch spool rotations during a trial, which could then be used to determine depth based on the radius dimension of the spool. Fundamentally, a Hall effect sensor is a device that detects the presence and strength of a magnetic field using the Hall effect—a phenomenon where voltage is generated across a conductor when it carries an electric current and is placed in a perpendicular magnetic field [1].

While the Hall effect sensor measured depth mechanically, the motor served as a generator to measure depth electrically. Although the motor powered the winch, it also served as a depth sensor through its generator-like properties. During the operation of raising the winch weight and pressure sensor apparatus, the motor delivered a measurable amount of output voltage. By applying Ohm's Law and the formula for electrical power, this output voltage could be expressed in terms of power [2]. Integrating power with respect to time yields energy, and a change in potential energy between the lowered and raised positions provides valuable information that can be leveraged to calculate depth displacement from the water surface to the ocean floor. In

[1]All authors are with the Department of Engineering, Harvey Mudd College, Claremont, CA 91711.

this way, all three sensors involved a winch to measure depth in distinct ways.

Accurate depth mapping in shallow recreational areas is important for safe navigation by boats and personal watercrafts. Current marine depth charts, such as those by iBoating, often lack high-resolution depth maps in regions near the shore [3]. This is especially relevant for areas near docks and beaches, where changing sediment patterns or man-made structures can alter underwater terrain. Thus, the intention of this project was to assess whether low-cost, multi-sensor systems mounted on an ASV could effectively collect data for small-scale environments near the shore.

The following report will detail the procedures applied to deploy the ASV and capture depth data using the three onboard sensors. It will also describe how each sensing method was calibrated and implemented. Following a detailed explanation of the sensor design and data collection procedures in the Experimental Setup section, the Results & Analysis section will compare outputs from each sensing method to evaluate their practicality and accuracy. Plausible sources of error will be examined in the Conclusion section in order to reflect on system limitations and propose improvements. Lastly, the report will summarize the main takeaways from this experiment and their implications for future development of depth-sensing ASV deployments in shallow recreational zones.

II. Experimental Setup

A. Engineering Goal

This project aimed to explore the viability of using electrical and mechanical depth measuring systems as an alternative to measuring depth through means of pressure. Since all three methods of capturing depth involved the same overall mechanical method of a winch weight being lowered from the ASV, it seemed reasonable to expect that all three methods would yield similar data. Nevertheless, it would be interesting to explore the ease of setup and calibration, accuracy, and cost effectiveness of the electrical motor and mechanical Hall effect depth measuring systems compared to the traditional pressure sensor.

Three distinct sensors were selected to measure depth: 1) Hall effect sensor (AH9246), 2) Motor (TRS-495SM), and 3) Pressure sensor (MPX5700). The microcontroller used to both activate sensors and collect data was the Teensy 4.0 (“Teensy”) developed by PJRC [4]. Importantly, the acceptable range for inputs into the Teensy analog pins is 0V to 3.3V [4]. The onboard power supply used for the project was an 11.1V LiPo battery pack [5] and the Motherboard (MTB) and custom PCBs were provided by the E80 course instructors [5].

B. Hall Effect Sensor Circuit Design

This particular AH9246 Hall effect sensor produced an active-low digital output that was equal in magnitude to its supply voltage (V_{CC}), which was set to 5V. Thus, the sensor had a quiescent voltage of 5V when far away from a magnet field and an active voltage of 0V when near a magnetic field. The intent was to shift this 0V-5V signal to be within the Teensy’s safe 0V-3.3V input range using a voltage divider. However, due to an implementation oversight, the unshifted 5V signal was connected directly through the MTB to Teeny analog PIN_A1. Although this exceeded the Teeny’s GPIO pin limit and introduced unnecessary risk, operation remained reliable and all components consistently functioned as expected during deployments. *Figure 2* below shows the circuit schematic for the Hall effect sensor. Furthermore, a MCP601 buffer op-amp was included to isolate the sensor output signal from the rest of the circuit to avoid loading and preserve signal integrity over noisy environments like Dana Point.

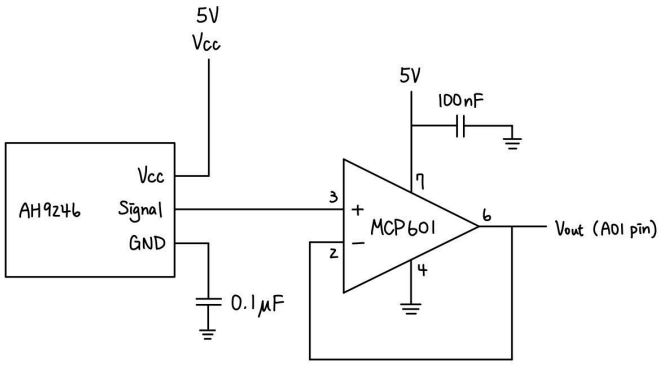

Figure 2: Circuit schematic of the AH9246 Hall effect sensor with a supply voltage of 5V and an MCP601 op-amp to prevent interferences to the signal due to loading.

To ensure proper function, the Hall effect sensor was orthogonally fixed 0.5cm away from a magnetic spot on the edge of the winch spool. In this way, when the winch lowered or raised, causing the spool to rotate, each full revolution would be recorded as a 0V voltage spike by the Hall effect sensor.

C. Motor-Based Sensor Circuit Design

The circuit design of the TRS-495SM motor aimed to serve two key purposes: 1) To function as an actuator that could raised the winch weight and pressure sensor system after being lowered, and 2) To support depth-sensing functionality through capturing change in voltage at the raised and lowered winch positions. The TRS-495SM brushed DC motor was selected for its compact form and torque characteristics suitable for raising the submerged winch weight [6].

Two unity gain buffer op-amps within a single MCP6002 chip were used to prevent impedance induced by the voltage dividers from affecting the cascade of follower op-amps shown in *Figure 3*. Following the buffers, the first MCP601 chip in the cascade was designed to be a differential op-amp—a type of amplifier that increases the difference between two input voltages [7]. This differential amplifier multiplied the voltage difference between the motor terminals (0.2V-0.4V) by a tenfold gain factor in order to increase the output voltage precision and sensitivity. Next, the signal was put through a second MCP601 chip which shifted the expected output range to 0.5V-3V, an input range suitable for Teensy analog PIN_A2. Notably, the motor was connected in parallel with the MTB and the circuit shown in

Figure 3. The MTB supplied 12V to the positive terminal of the motor.

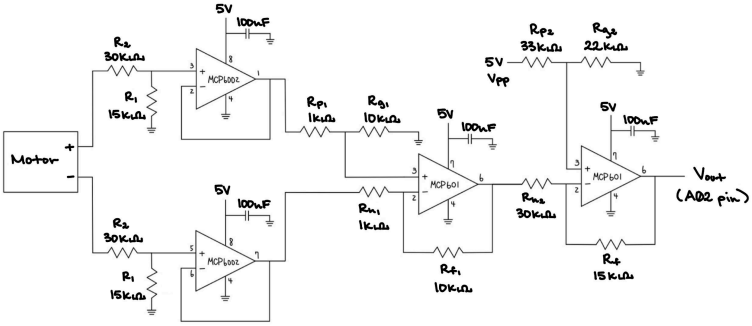

Figure 3: Circuit schematic of the TRS-495SM motor sensor in which MCP6002 op-amps act as unity gain buffers. A first MCP601 is used as a differential op-amp to amplify voltage difference between motor terminals and a second MCP601 is used to shift the signal into Teensy range (0.5V-3V).

D. Pressure Sensor Circuit Design

The standard method for determining water depth throughout the E80 course was via a MPX5700 pressure sensor—a piezoresistive analog sensor capable of measuring differential gauge pressure up to 700kPa [8]. From the pressure sensor datasheet, it was found that a voltage output range from 0.8V-1.3V was expected from a given water surface to a depth of 5m [8]. As a result, the following circuit schematic shown in *Figure 4* was designed to improve signal precision while safely interfacing with the Teensy. The first MCP601 was configured as a unity gain buffer to prevent signal interference from loading. The second op-amp was used to amplify and shift the 0.8V-1.3V signal to a range of approximately 0.4V-2.9V, improving resolution while remaining within the Teensy's safe voltage limits. Moreover, resistor values of R_p = 100kΩ and R_g = 30kΩ were selected to offset the amplified signal by 1.15V, effectively centering the signal in Teensy range. Additionally, R_n = 10kΩ and R_f = 47kΩ were selected to set the gain of the non-inverting amplifier to 5.7, enabling more fine resolution for small pressure changes while avoiding railing out. The buffered and scaled signal was then fed into Teensy analog PIN_A0.

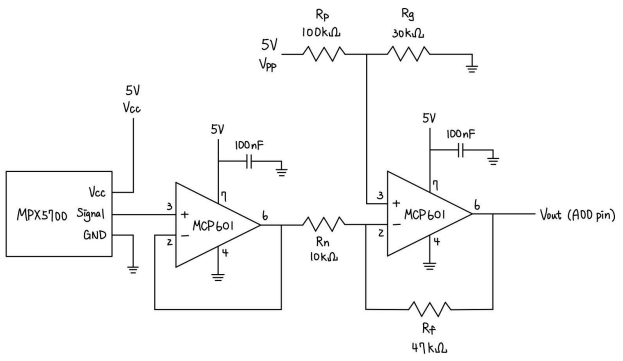

Figure 4: Circuit schematic of the MPX5700 pressure sensor in which two MCP601 op-amps cascade to prevent loading impedance and shift the signal into Teensy range (0.4V-2.9V).

E. Mechanical Design

Winch weight selection depended both on mass and shape. A steel plate with dimensions 2in x 2in x 0.5in was identified to be the optimal weight and shape. Weighing approximately 200g, the steel plate met the weight threshold to fully and continuously rotate the winch spool under the downward force of gravity and upward force of water buoyancy. Through experiments conducted in the Harvey Mudd College Tank Room to raise the steel plate using the winch, it was determined that the motor was easily able to generate sufficient torque to lift this weight. In terms of shape, it was found that a plate like this—with a non-trivial amount of thickness and a large surface area—was optimal for being caught by the electromagnet as well as for forming a sufficiently strong connection to stay in place during movement between trials.

A hole was drilled through the steel plate, through which the free end of fishing line coiled around the winch spool was threaded. The free end of the fishing line was then hot glued to a nut, mechanically preventing the plate from disconnecting from the end of the fishing line. As shown in *Figure 5* below, the open end of the pressure sensor tube was put through the nut and glued in place. In this way, the winch weight would be capturing data at the same depth as the pressure sensor for each trial.

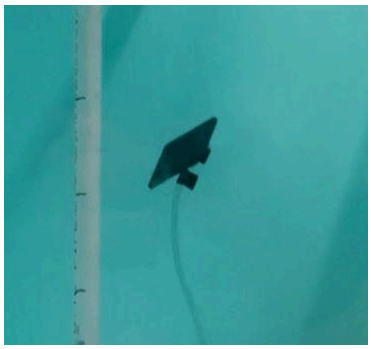

Figure 5: The steel plate winch weight falls under the force of gravity. The open end of the pressure sensor is mechanically attached to the weight such that the winch measuring systems and pressure sensor system all measure depth at the same location.

Another critical mechanical consideration was the placement of the Hall effect sensor relative to the electromagnet since the former is a device that reads magnetic fields and latter is a device that can switch on or off a magnetic field. The Hall effect sensor was fixed perpendicularly within the robot's PVC frame at a distance 0.5cm from the magnets embedded in the edge of the winch spool. Below, *Figure 6a* at left shows the placement of the Hall effect sensor relative to the winch and *Figure 6b* at right shows the placement of the magnets inside the shoulder of the spool. Notably, a stack of 8 magnets was used in order to create a sufficiently strong magnetic field to trigger the Hall effect sensor consistently.

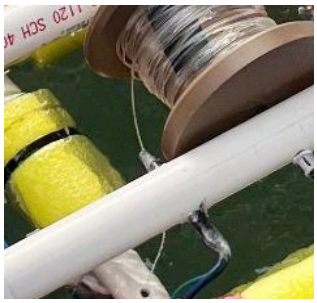

Figure 6a (left): The waterproofed Hall effect sensor is oriented perpendicular to the magnets and sits a distance of 0.5cm from the spool.

Figure 6b (right): A stack of 8 disk-shaped magnets are glued into the winch spool shoulder to activate the Hall effect sensor once per full rotation.

To best orient the electromagnet to catch the winch weight as well as prevent it from accidentally triggering the Hall effect sensor, the electromagnet was placed facing downwards, beneath the robot and directly in line with the path of the fishing line. *Figure 1* shown previously presents the orientation of the electromagnet at a position that is both far away and facing away from the Hall effect sensor.

Also important was ensuring that the ASV could float and that activation of the winch would not significantly rock the robot back and forth. To overcome these potential issues, the ASV was designed to be wide and relatively flat in accordance with Archimedes' Principle which states increasing surface area of a floating body enables it to displace more water, consequently increasing its upward buoyant force making it float higher and be more stable [9]. Furthermore, designing a wider base also improved resistance to tilting since a wider base requires more torque to be tilted. Considering the above objectives, the ASV was designed to measure 2.5ft in length, 3ft in width, and 1.5ft in height. To counteract the approximate 15lb weight of the robot equipped with all components, buoyant pool float supports were added along the bottom level of the robot's frame. The two heaviest components—the winch and the electronics housing box—were optimally determined to be placed near the center of the ASV to reduce pitch-roll torque and improve stability, and on opposite sides to ensure lateral balance, keeping the robot level and stable in the water [10]. *Figure 7* shows the mechanical setup of the ASV.

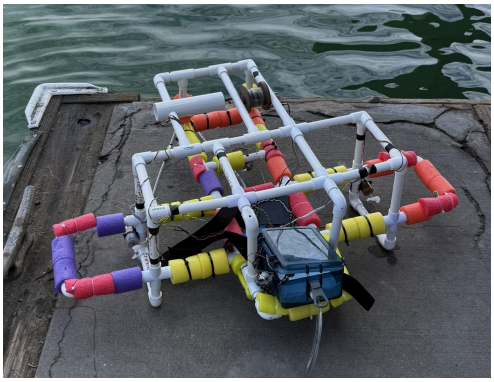

Figure 7: The arrangement of the winch, electronics housing box (transparent blue box), sensors, and buoyant pool float supports are shown on the ASV. The housing box is open and outside of the robot frame so that new code may be uploaded to the Teensy. A waterproofed motor was placed on either side of the robot to control navigation.

A final mechanical concern was waterproofing all components to prevent water intrusion that could damage the electronics and compromise function. This was addressed by enclosing the Arduino, battery, and MTB inside a sealed housing box. Cable penetrations into this housing were sealed using epoxy-filled penetrators, which provided a durable and watertight barrier. For exposed wiring connections, heat-shrink tubing was applied to ensure tight insulation. Additionally, Parafilm was wrapped around the external connectors as a secondary layer of moisture protection. These combined methods helped ensure that the ASV remained safe in wet environments.

F. Experimental Procedure

The selected ASV design was a surface navigating robot which would move autonomously on water surfaces and use P-control to reach specified 2D waypoint locations [11]. Upon reaching a waypoint, the robot was designed to hold its position and deactivate the electromagnet in order to allow the winch weight and pressure sensor apparatus to lower to the ocean floor by gravity. After a brief pause, the TRS-495SM motor would fire to raise the weight and pressure sensor. Simultaneously, the electromagnet would reactivate in order to catch the steel weight and lock it in the raised position. Once connected, the robot's driving motors would turn on to maneuver the ASV to the next waypoint for another trial.

The order of operations for a given trial can be broken down into four phases that repeat until reaching the final desired 2D surface position: 1) Drive to a waypoint, 2) Lower winch, 3) Hold idle, and 4) Raise winch. The steps for collecting data can be expressed in the form of states in a finite state machine (FSM)—a system that transitions from one singular state to another in response to an input. During each phase or state, the code was set to execute specific actions by each component in a specified order. *Figure 8* provides a visual for the order of operations for a given trial and which components are active (1) or inactive (0) during a particular state. Transitions between states are written as descriptions but were mathematically coded using Arduino IDE software which is a variation of C++. A delay of 2 seconds between Hall effect activations was selected as a method for determining when the winch spool had stopped rotating and a cue that S2→S3. If no rotations were to occur over a 2 second span, it is assumed that the winch weight must have reached the ocean floor, no longer able to induce a torque on the spool. To add, a delay of 2 seconds was selected between S3→S4 to allow sufficient time for the pressure sensor to settle into a stable reading. A delay of 10 seconds was selected between S4→S1 to allow sufficient time for the winch to raise the weight and pressure sensor apparatus.

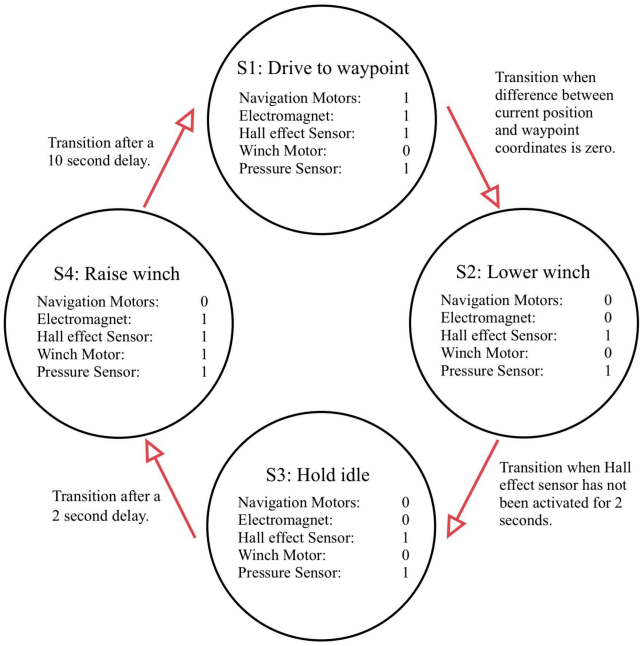

Figure 8: FSM diagram that represents the four phases required to collect depth data for a given trial. Components are either active (1) or inactive (0) depending on the state.

III. Results & Analysis

A. Deployment Overview

On April 26, 2025, the ASV was deployed from the Baby Beach dock to shore at Dana Point Harbor, CA. The morning was spent recalibrating hard iron and soft iron coefficients for the magnetometer—an instrument that measures changes in the Earth's magnetic field and can be used to determine the global orientation of the robot [12]. For the majority of the day, it was cloudy out with several instances of fast winds and heavy rainfall. While the three sensor mechanisms were able to be tested in the Harvey Mudd College Tank Room and the arrival at waypoints correctly triggered the release of the winch weight and pressure sensor apparatus, the surface navigation and control systems were not tested in aquatic environments prior to deployment at Dana Point.

At Dana Point, the robot was unable to autonomously navigate to waypoints. Hours were spent debugging the code, but the autonomous navigation remained unsuccessful. To remedy this issue, it was decided that the ASV would need to be manually moved along the water surface from position to position between the harbor dock and shoreline. In order to properly implement the solution, the Arduino code used to control the navigating motors on the sides of the robot were disabled. Additionally, code to interface the sensors was modified to deploy every 60 seconds instead of when the ASV reached a specified 2D waypoint location. Due to limited time with the rented kayaks, Simone Yang, a student team member, entered the harbor water and manually swam to move the robot along a path due North from the dock to the shoreline.

B. Sensor Comparison

To assess the reliability and accuracy of the three different depth-sensing methods integrated on the ASV, a side-by-side comparison was conducted using the data collected during the Dana Point Harbor deployment. The three sensors—Hall effect sensor, motor energy consumption, and pressure transducer—each rely on different physical principles to estimate the depth reached by descending a steel weight connected to a winch mechanism. To produce a consistent and interpretable depth profile across sensor types, each form of raw data was cleaned, calibrated, and plotted against the distance from shore where each point was collected.

The Hall effect sensor counted the number of digital state transitions (HIGH to LOW) as magnets embedded in the winch spool shoulder passed by the sensor fixed in the robot's frame. Since one HIGH-LOW or LOW-HIGH transition corresponds to half a rotation of the spool, the number of total transitions was divided by two and then converted to a linear depth using the formula for arc length shown in *Equation 1*. In this equation, $Depth_{Hall}$ is the depth estimation of the Hall effect sensor in meters and D represents the diameter of the winch spool which was 5.5cm. Moreover, $Number\ of\ Transitions$ is the integer number of changes between HIGH-LOW or LOW-HIGH readings by the Hall effect sensor for a given trial as the winch spool lowered.

$$Depth_{Hall} = (Number\ of\ Transitions) \times \frac{\pi \cdot D}{2} \qquad (1)$$

The motor-based method for measuring depth relied on integrating the square of the voltage across the winch motor over time—a value that was empirically found to be proportional to energy input, assuming constant resistance. This input energy reflects the total work done by the motor to raise or lower the winch weight. During calibration in the Harvey Mudd College Tank Room, known depths were associated with their corresting integrated motor voltage squared values, allowing a linear regression to be fit. The calibration curve, shown in *Equation 2*, maps motor energy input to meters in depth , where $V_{Motor}^{\ 2}$ is the integrated motor voltage squared in arbitrary Teensy Units (TU) and the constants were derived from a best-fit regression.

$$Depth_{Motor} = 0.00051116 \cdot V_{Motor}^{\ 2} - 0.767771 \qquad (2)$$

The pressure sensor method provided a direct physical measurement of depth based on hydrostatic pressure. The sensor outputs analog voltages corresponding to ambient water pressure, which decreases linearly with depth since an inverting op-amp circuit was used. To convert this to depth in meters, a linear calibration was conducted using two known pressure-depth pairs collected at Dana

Point: one at a depth of 0m at the surface and one at a measured depth of 3.07m at the dock. Using these reference points, a line of best fit was generated and is expressed in *Equation 3*. This equation presents the relationship between depth $Depth_{Pressure}$ in meters estimated by the pressure sensor as a function of $V_{Pressure}$ which represents output voltage in TU from the pressure sensor. Values of $V_{Pressure}$ were determined from the raw data. Since the winch weight and pressure sensor apparatus remained idle in S3 for 2 seconds before being raised, the collected data shows a stable, horizontal line of where the pressure was constant at the ocean floor of a particular waypoint. The pressure sensor voltage during this time was averaged to obtain $V_{Pressure}$.

$$Depth_{Pressure} = -0.487302 \cdot V_{Pressure} + 37.57095 \quad (3)$$

The raw data from all three sensor systems is visualized in *Figure 9*, which shows the original TU output of each method without calibration applied. This plot highlights how different the unprocessed signals are and helps illustrate why scaling and calibration are necessary in order to compare measurement methods. Notably, the axes were kept in Teensy Units (TU) for output voltage and Teensy Sampling Units (TSU) to maintain accuracy. During steps to clean the data, it was found that scaling TU into voltage in volts and time in seconds led to a severe loss of precision due to rounding errors by MATLAB processing software. As a result, all internal units—arbitrary units shared between inputs and outputs—remained in terms of TU for both output voltage and time.

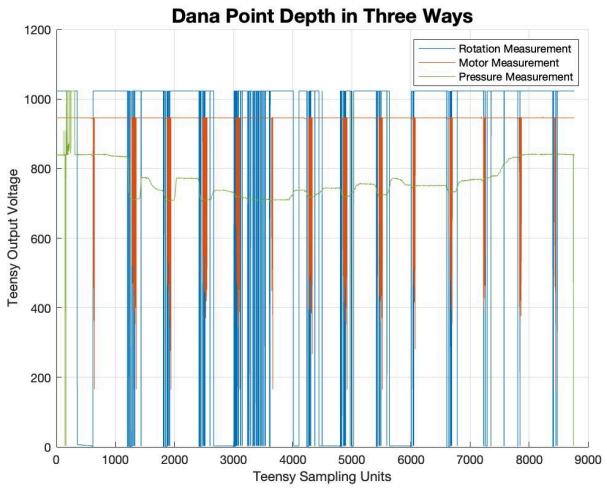

Figure 9: Raw sensor data from Hal effect transitions, motor output, and pressure sensor. The y-axis is in Teensy Unit output voltage while the x-axis is in Teensy Sampling Units (TSU).

Since position along the water surface in meters and as well as TU output voltage by all sensors were sampled in TU portions of time (TSU), matching GPS position and Teensy outputs for a given trial could enable a direct comparison between position along the surface path in meters and water depth in meters for a given time. As previously mentioned, *Equations 1-3* were used to convert sensor output information directly to water depth in meters. Depth and position from the shore to the dock were plotted against each other and the results are shown in *Figure 10*. Notably, trial 1 (700TSU) of the uncalibrated data shown in *Figure 9* was excluded from analysis because the robot was not yet in the water. Additionally , trial 6 (3500TSU) shown in *Figure 9* was also excluded because the winch weight did not make full contact with the electromagnet and proceeded to lower unintentionally. Thus, the data plotted in *Figure 10* shows only the 11 points that were identified to be viable. Visually, the path along which Simone Yang manually moved the robot is shown in *Figure 11*.

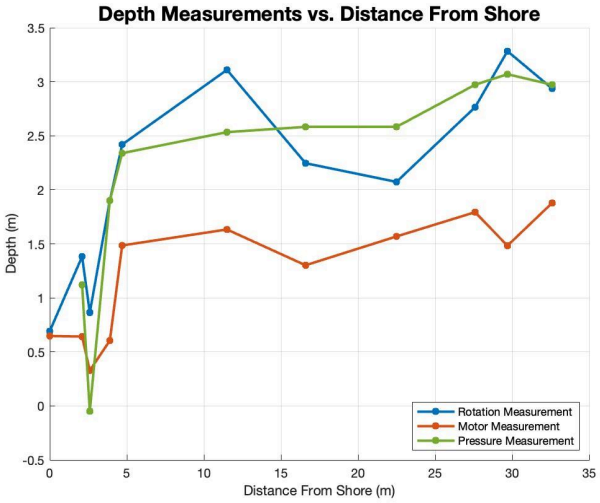

Figure 10: In meters, calibrated depth estimations for each sensor are plotted against the robot's distance from the shore for a given trial. A total of 11 viable trials were taken.

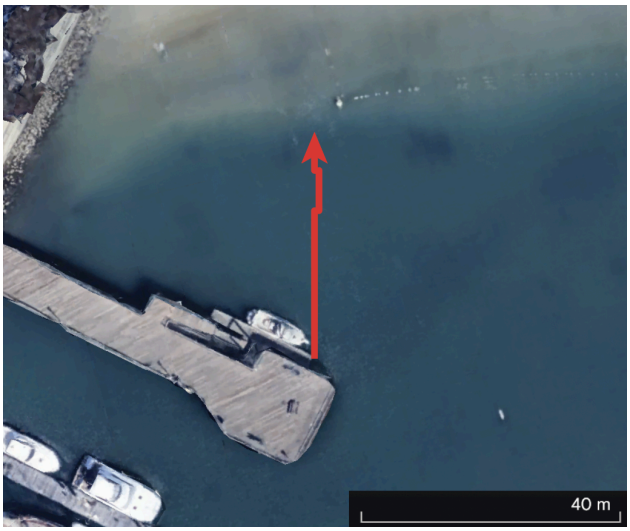

Figure 11: An image of the route Simone Yang took to navigate the robot. The path is approximately 40m due North.

IV. Conclusion

A. Significance of Results

The deployment and testing of three distinct depth sensing mechanisms—Hall effect sensor, motor-based voltage sensor, and pressure sensor—provided multiple complementary perspectives on underwater depth measurement for an autonomous surface vehicle. While each method exhibited specific strengths and weaknesses, their collective analysis allowed for valuable cross-verification and insight into system behavior under real-world conditions.

Although *Figure 10* shows a similar trend across measuring methods where depth initially increases rapidly with distance from the shore and then levels off, exact values vary. To quantify the degree of variation between depth estimation by each sensor, paired t-tests were conducted. A first paired t-test revealed no statistically significant difference between the pressure and Hall effect sensor measured data ($P = 0.742$). A second t-tests revealed the motor and Hall effect sensor data were statistically different ($P = 2.06 \times 10^{-5}$) and so were the motor and pressure sensor data ($P = 2.49 \times 10^{-4}$).

When compared to ground truth depth measurements collected at the dock, the pressure sensor proved most accurate, with the Hall effect sensor yielding similar values. Given the significant deviation from the motor data, however, it cannot be concluded that the motor-based voltage method accurately reflects true water depth. Ultimately, these findings validate the reliability of the pressure and Hall effect sensors for use in shallow water depth mapping on low-cost ASVs, while highlighting the need for improved calibration and modeling if the motor-based method is to be used for depth sensing in non-ideal aquatic environments.

The pressure sensor offers a direct measurement of depth based and is commonly used in underwater sensing. However, its performance was affected by multiple issues during deployment. Sand was discovered inside the open end of the pressure tube after field testing, which could have disrupted pressure readings, by blocking water from fully entering the tube. This error could have caused the sensor to not register the full water pressure which could lead to an underestimation of depth. Since measurements started at the dock and went towards the shore, the final trials near the beach could have accumulated sand which could explain the low pressure sensor depth readings at locations 0-5m from the shore. Additionally, while the open end of the MPX5700 pressure sensor tube was fixed to the winch weight, the rest of the tube was left dangling in the water, weighed down by small interspaced weights. Given the unpredictability of an ocean environment, the pressure sensor tube could have experienced bends or kinks due to its own weight that could have compressed the tube unexpectedly, leading to inconsistent or erratic pressure readings.

The Hall effect sensor recorded magnetic transition as the winch spool rotated, assuming smooth, one-directional movements for either raising or lowering operations. It operated well under ideal conditions but could have exhibited weakness during real-world testing. Notably, the sensor simply counted HIGH-LOW or LOW-HIGH transitions, and strong waves could have caused the winch spool to momentarily reverse direction. This could have unintentionally triggered the sensor in reverse, and falsely increased the rotation count. These events could have led to an overestimation of depth at the location 11m from the shore, for example.

The motor voltage method used the motor as both an actuator and generator during retrieval of the winch weight. Voltage output changed as the winch weight was pulled upward, offering a substitute for mechanical energy expended. However, this method had a major limitation in calibration. The calibration curve for the motor was developed in a still-water tank environment, which allowed for clear visualization of the weight at the bottom of the tank but lacked real-world disturbances like waves, seaweed, or varying drag. As a result, the voltage-depth relationship during deployment may have differed substantially, introducing systematic error that would explain the consistently lower motor depth estimation from distances 5-35m from the shore. Furthermore, without real-time current measurement, assumptions made about power may have oversimplified actual motor behavior under a load.

B. Future Work

There are several directions for improving and expanding upon the work done in this project. One key improvement would involve redesigning the pressure sensor tube system to ensure greater reliability. The robot was originally designed to use a SEN0257 which can measure water pressure without the use of a sensitive tube that connects back to the Teensy [13]. Before the Dana Point deployment, the SEN0257 sensor was discovered to be non-functional. However, with more time, future designs for the ASV would incorporate a more practical sensor like the SEN0257 that cannot get severely clogged and are unaffected by kinks since they do not require a tube back to the Teensy.

To remedy the issue of wave-induced spool jerks that falsely trigger the Hall effect sensor, a slower and more controlled descent of the winch weight could be implemented to reduce sudden motions. Additionally, placing magnets more frequently at evenly spaced intervals around the spool would improve resolution and help distinguish between valid and erroneous rotations counts of the spool.

A future version of the project should include dynamic calibration trials in open water locations such as the Bernard Field Station to better test for real-world factors that the motor sensing method would encounter [14]. Notably, the robot was not prepared in time to be tested at the Bernard Field Station as intended. Had the robot been tested outside

in water as intended, issues with the surface control and navigation code could have been solved before arriving at Dana Point. Additionally, future work might also include more precise sampling of motor voltage and current which could help improve fundamental understanding of energy-based depth estimation.

This project demonstrated the value of combining multiple sensing systems to assess underwater depth from an ASV. Through the process of mechanical integration, sensor calibration, and time-limited field deployment, valuable lessons in design decisions and how real-world environment factors shape data reliability were learned. While the pressure and Hall effect sensors produced consistent and comparable depth measurements, the motor-based method proved less accurate in dynamic conditions which highlights the importance of calibrating sensors in their intended environments. Ultimately, this work highlights that even low-cost sensor systems can yield useful depth data when thoughtfully designed and cross-validated.

Acknowledgments

The team would like to thank Prof. Helmns, Prof. Brake, and Prof. Yang for their guidance as course instructors. Additionally, this project would not have been possible without the contributions from Engineering Staff Lynn Kim, Xavier Walter, and Jacob Stimpel. Lab Proctors Naomi, Kayla, Jasper, Katrina, and Gina were incredibly helpful in providing design suggestions, debugging advice, and reopening the lab at late hours. To add, Nina Jobanputra and Sheridan Dorsey shared valuable insights from previous projects on designing winch-based systems. Lastly, the team would not have been able to collect data without the Hall effect sensor generously given to us by Team 31 (Christian Lam-Alvarez, Ivy McFetridge, Micah Borge, and Sophie Khuu).

References

1. Texas Instruments, “SSZT164: Application of Hall Sensors in Brushless DC Motor Control,” *TI.com*. [Online]. Available: https://www.ti.com/document-viewer/lit/html/SSZT164.
2. “DC Circuit Examples,” *Electronics-Tutorials.ws*. [Online]. Available: https://www.electronics-tutorials.ws/dccircuits/dcp_2.html.
3. “Dana Point Harbor Nautical Chart US18746,” *GPS Nautical Charts*. [Online]. Available: https://www.gpsnauticalcharts.com/main/us18746_p1898-dana-point-harbor-nautical-chart.html.
4. PJRC, “Teensy 4.0,” *pjrc.com*. [Online]. Available: https://www.pjrc.com/store/teensy40.html.
5. Harvey Mudd College, “Lab 0: Batteries,” *HMC E80 GitHub Pages*. [Online]. Available: https://hmc-e80.github.io/labs/lab0/index.html#battery.
6. Tsinymotor, “Mini DC Motor,” *tsinymotor.com*. [Online]. Available: http://www.tsinymotor.com/Products/DC_Motor/2014/0516/46.html.
7. “Op-Amp Comparator Circuits,” *Electronics-Tutorials.ws*. [Online]. Available: https://www.electronics-tutorials.ws/opamp/opamp_5.html.
8. NXP Semiconductors, “MPX5700: Pressure Sensor Datasheet,” *NXP.com*. [Online]. Available: https://www.nxp.com/docs/en/data-sheet/MPX5700.pdf.
9. “Archimedes' Principle,” *Encyclopædia Britannica*. [Online]. Available: https://www.britannica.com/science/Archimedes-principle. [Accessed: May 9, 2025].
10. “Center of Gravity and Buoyancy,” *EngineeringToolbox.com*. [Online]. Available: https://www.engineeringtoolbox.com/centre-gravity-buoyancy-d_1286.html.
11. Harvey Mudd College, “Navigation,” *HMC E80 Project Site*. [Online]. Available: https://hmc-e80.github.io/project/navigation/.
12. NOAA, “Magnetometers,” *NOAA Ocean Explorer*. [Online]. Available: https://oceanexplorer.noaa.gov/technology/magnetometer/magnetometer.html.
13. DFRobot, “Gravity: Analog Water Pressure Sensor,” *Digi-Key*. [Online]. Available: https://mm.digikey.com/Volume0/opasdata/d220001/medias/docus/2194/SEN0257_Web.pdf.
14. Friends of the Ballona Wetlands, “About Us,” *fbbfs.org*. [Online]. Available: https://www.fbbfs.org/about.html.